RESEARCH ARTICLE

Assessing vertical diffusion in a stratified lake using a three-dimensional hydrodynamic model

Fei Dong[1,2*] | Chenxi Mi[2,3*] | Michael Hupfer[4] | Karl-Erich Lindenschmidt[5] | Wenqi Peng[1] | Xiaobo Liu[1] | Karsten Rinke[2]

[1]State Key Laboratory of Simulation and Regulation of Water Cycle in River Basin, China Institute of Water Resources and Hydropower Research, Beijing, China

[2]Helmholtz Centre for Environmental Research, Department of Lake Research, Magdeburg, Germany

[3]College of Water Conservancy, Shenyang Agricultural University, Shenyang, China

[4]Department of Chemical Analytics and Biogeochemistry, Leibniz-Institute of Freshwater Ecology and Inland Fisheries, Berlin, Germany

[5]Global Institute for Water Security, University of Saskatchewan, Saskatoon, Saskatchewan, Canada

Correspondence
Chenxi Mi, Helmholtz Centre for Environmental Research, Department of Lake Research, Magdeburg, Germany.
Email: chenxi.mi@ufz.de

Abstract

Vertical turbulent diffusivity (K_z), which can be estimated from water temperature, is a key factor in the evolution of water quality in lentic waters. In this study, we analysed the capability of a three-dimensional hydrodynamic model (EFDC) to capture water temperature and vertical diffusivity in Lake Arendsee in the Northern German plain. Of particular interest to us is to evaluate the model performance for capturing the diffusion minimum within the metalimnion and analyse the response of the metalimnetic K_z to meteorological forcing, namely changing wind speed and warming. The comparison confirmed that the calibrated model could reproduce both stratification dynamics and vertical diffusion profiles in the lake. The model was also shown to be able to capture the duration and vertical extent of the metalimnetic diffusion minimum. The scenario results illustrate that, compared to air temperature, wind velocity appeared to be the more influential meteorological variable on the vertical exchange within the metalimnion. While increasing wind velocities mostly affected the minimum values of K_z in the metalimnion and thus led to intensified vertical exchange, the reduction of wind velocity mostly affected the depth of minimal K_z, but not its absolute value.

KEYWORDS

climate change, EFDC, Lake Arendsee, stratification dynamics, vertical turbulent diffusivity

1 | INTRODUCTION

Thermal stratification is a key feature in many lentic waters such as lakes and reservoirs (Boehrer & Schultze, 2008). During warm seasons, surface waters heat up and have a lower density than the colder deeper waters. The two layers are separated by the metalimnion, a distinct zone with steep temperature (thermocline) and density gradients. Given the fact that lakes are most abundant between

subarctic and Mediterranean climates (Lehner & Döll, 2004; Pekel, Cottam, Gorelick, & Belward, 2016), that is, in a seasonal temperature regime that strongly supports the occurrence of thermal stratification, the vast majority of lakes undergo some degree of thermal stratification. In a stratified lake, the intensity of vertical mixing, expressed as the vertical turbulent diffusion coefficient K_z, is typically high in the epilimnion (often more than $10^{-4} m^2 s^{-1}$) because of wind stirring and convection, and much lower in the hypolimnion (usually less than $10^{-5} m^2 s^{-1}$) where internal waves (e.g. Boehrer, 2000; Boehrer, Ilmberger, & Münnich, 2000), bottom friction and shear drive turbulent mixing (Goudsmit, Peeters, Gloor, & Wüest, 1997; Valerio, Pilotti, Marti, & Imberger, 2012; Wüest & Lorke, 2003). The layer in between, that is, the metalimnion, is characterized by extremely low vertical mixing because of its strong density gradient. This makes the metalimnion a separate layer where local phenomena can persist for a long time before being dispersed by a large mixing event. Examples of such phenomena within the metalimnion are chlorophyll maxima (Leach et al., 2018), oxygen maxima (Wilkinson, Cole, Pace, Johnson, & Kleinhans, 2015) or oxygen minima (Kreling et al., 2017; Wentzky, Frassl, Rinke, & Boehrer, 2019).

The consequences of stratification are multifaceted, affecting physical, chemical and biological processes in several ways (Luo et al., 2018; Yang et al., 2018). Most importantly, the temperature and density gradients along the vertical axis suppress vertical exchange between the epilimnion and hypolimnion and thus give rise to the formation of chemical gradients (e.g. Dietz, Lessmann, & Boehrer, 2012) or oxyclines (Boehrer & Schultze, 2008). Atmospheric oxygen cannot replenish the hypolimnetic oxygen deficit because of the mixing barrier of the metalimnion (Fenocchi et al., 2019). Phytoplankton, on the other hand, often profit from stratification because the reduced vertical mixing protects algal cells from being mixed down into dark layers where low light conditions limit photosynthesis. In many deep lakes, therefore, algal growth can only start once stratification is established and algal cells remain suspended within the epilimnion (Peeters, Straile, Lorke, & Ollinger, 2007; Sommer, Gliwicz, Lampert, & Duncan, 1986).

Stratification models have been developed for more than 30 years (Imberger, 1981; Riley & Stefan, 1988). Meanwhile, temperature variations, both in depth and time, achieve high coefficients of determination in many cases (often above 95%, see Arhonditsis & Brett, 2004; Mi, Frassl, Boehrer, & Rinke, 2018) when simulations are compared with observed data as several model tools and case studies have described (e.g. Frassl et al., 2018; Mi, Sadeghian, Lindenschmidt, & Rinke, 2019; Perroud, Goyette, Martynov, Beniston, & Anneville, 2009; Wahl & Peeters, 2014). Since water temperature variability over a season is very high in the epilimnion and comparatively low in the hypolimnion, the high model performance for temperature dynamics of existing models mostly reflects their excellent ability to simulate temperature dynamics in the surface layers. In that sense, model skill estimates like RMSE or R^2 are biased if they incorporate all values aggregated over the whole depth range. These dynamics are strongly controlled by meteorological variables and therefore largely a direct response to the input data (Woolway & Merchant, 2017). The direct effect of meteorological

drivers, however, diminishes with depth and below the thermocline, their contribution to mixing is only indirect.

In fact, many models show small but systematic differences in simulated hypolimnion temperatures (e.g. Perroud et al., 2009). Stepanenko et al. (2010) even concluded, in a comparison study of 1D lake models, that temperature dynamics below the thermocline are notoriously difficult to simulate. This limitation is a consequence of the fact that turbulent kinetic energy in the hypolimnion is mostly created by the dissipation of basin scale internal waves, that is, a 3D process, and therefore cannot be properly mimicked in a 1D approach. Although existing 1D models are undergoing further improvements in order to account for effects from basin scale internal waves (Gaudard et al., 2017; Yeates & Imberger, 2003), we usually expect better performance from a 3D model, compared to a 1D model, with respect to hydrodynamics simulation in the hypolimnion. Our study was motivated by the question of how well a 3D hydrodynamic model is able to reproduce vertical transport beneath the surface layer, that is, within the metalimnion and the hypolimnion of a deep, stratified, temperate lake. For this purpose, we chose a lake with simple basin morphometry and only marginal hydrological forcing, but with pronounced gradients and distinct physicochemical patterns along the vertical axis.

Unlike most other studies using hydrodynamic models, we do not only use the dynamics of water temperature (i.e. a model state variable) for model assessment but also explicitly check its abilities on the process level by comparing observed and simulated vertical diffusivity (i.e. a process) quantitatively. We believe that this is a more informative approach because any deviation on the level of the model states is not necessarily informative regarding the corresponding deviation of the involved processes due to nonlinearities and nonadditive interactions with other processes. We therefore followed the concept established in Wahl and Peeters (2014), who also used a 3D model for comparing observed and simulated vertical diffusivity in deep Lake Constance. We extended their study by (a) including a detailed analysis of vertical diffusivity within the metalimnion, (b) designing a detailed field program using high-resolution monitoring, and (c) applying a high spatial resolution in the model grid in order to better resolve 3D effects.

The focus of this study is on a tight combination of a 3D hydrodynamic model application and in situ measurements related to vertical mixing in a large and stratified lake. The major novelty of our study is the detailed investigation of the diffusion minimum in the metalimnion of a deep lake using a combination of high-frequency in situ measurements and 3D modelling, as well as the sensitivity of this diffusion minimum to external forcing from wind and air temperature. Unlike other modelling studies, we are not focusing our analysis on comparing model states (e.g. water temperature) but on the comparison of key characteristics at the process level (e.g. vertical turbulent diffusion). We pursued the following three research objectives: (a) establish a detailed, high resolution field monitoring program for water temperature in order to calculate turbulent vertical diffusion coefficient K_z with the gradient flux method (Heinz, Ilmberger, & Schimmele, 1990), (b) perform simulations with a 3D lake model and derive lake-wide estimates of modelled turbulent vertical diffusion, and (c) analyse the turbulent vertical diffusion within the metalimnion

and its sensitivity to the meteorological drivers (i.e. air temperature and wind velocity).

2 | MATERIALS AND METHODS

2.1 | Study site

Lake Arendsee is a dimictic temperate lake located in the North German Plain (55°53′21″N, 11°28′27″E, 23.3 m above sea level). The lake originated from a collapsed salt doline, has an elliptical shape, a surface area of 5.14km² and maximum and mean depths of 49.5 and 29 m, respectively (Figure 1). The littoral zone is relatively steep and the cross-sectional area at 30 m depth is 3.07 km². The hard-water lake is mainly fed by groundwater. Currently, four ditches drain adjacent agricultural fields into the lake and a small artificial runoff channel transports water out of the lake. The theoretical water residence time is between 50 and 60 years (Meinikmann, Hupfer, & Lewandowski, 2015). The above-ground catchment area (29.5 km²) is dominated by agriculture (52.1%) and forestry (30.6%). The town of Arendsee is situated directly on the south-west shore. At least since the middle of the last century, the lake has been strongly eutrophied. High total phosphorus concentrations (2013–2017: 0.19 mg L^{-1} on average) often lead to low transparency depths (ca. 1 m) due to the mass development of phytoplankton during the vegetative period. The phytoplankton is dominated by cyanobacteria such as *Planktothrix rubescens*; or diazotrophic *Anabaena flos-aquae*, and *Aphanizomenon flos-aquae*. Dissolved oxygen (O_2) in the hypolimnion at the end of summer stratification has continuously decreased over the last four decades. During summer stratification a distinct metalimnetic oxygen minimum extending several meters is formed every year. More detailed information on the lake origin, morphometry, hydrological regime and physical properties may be found in Findlay, Kling, Rönicke, and Findlay (1998), Hupfer, Reitzel, Kleeberg, and Lewandowski (2016), Engelhardt and Kirillin (2014) and Bernhardt and Kirillin (2013).

2.2 | Numerical model

The 3D model of Lake Arendsee was established using the environmental fluid dynamic code (EFDC, the utilized distribution is EFDC Explorer Release 8.2.5, DSI LLC), a public domain, open source, surface water modelling system that can be downloaded at https://www.epa.gov/exposure-assessment-models/efdc. EFDC includes routines for 1D, 2D, and 3D hydrodynamics with module extensions for various processes, such as sediment transport, ecosystem dynamics, submerged aquatic vegetation and sediment diagenesis (Hamrick, 1992). EFDC was originally developed at the Virginia Institute of Marine Science and the School of Marine Science in the College of William and Mary in Virginia (Tetra, 2007). EFDC has been applied to more than 100 water bodies including rivers, lakes, reservoirs, wetlands, estuaries, and coastal ocean regions for environmental assessment and
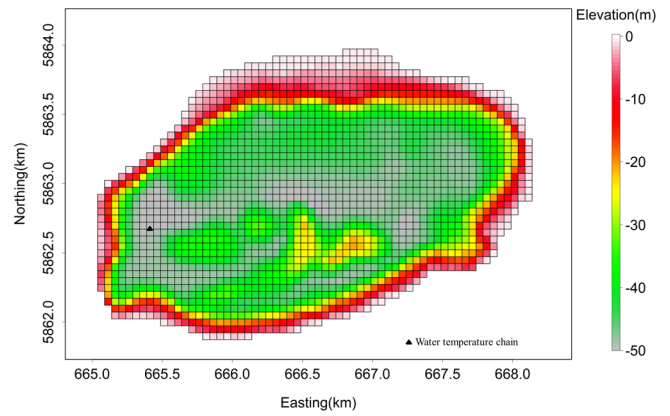

FIGURE 1 Model grid of Lake Arendsee used in the simulations, the horizontal resolution is 50 × 50 m². The colour scale represents the maximum depth in each grid cell. The black triangle marks the location of sampling point (temperature chain). Coordinates are given in UTM

management. It is recommended by the US EPA as a standard 3D hydro-environmental simulation tool (Wang, Li, Jia, Qi, & Ding, 2013; Wu & Xu, 2011). EFDC uses a three time level, finite difference scheme with an internal–external mode splitting procedure to separate the internal shear or baroclinic mode from the external free surface gravity wave or barotropic mode. The vertical diffusion coefficients for momentum, mass and temperature are determined by the turbulent closure model of Mellor and Yamada (1982), which involves the use of analytically determined stability functions and the solution of transport equations for the turbulence intensity and length scale (Hamrick, 1996).

The momentum and continuity equations and the transport equations for salinity and temperature are shown below (Hamrick, 1992):

$$\frac{\partial(mHu)}{\partial t} + \frac{\partial(m_y Huu)}{\partial x} + \frac{\partial(m_x Hvu)}{\partial y} + \frac{\partial(mwu)}{\partial z} - Hv\left(mf + v\frac{\partial m_y}{\partial x} - u\frac{\partial m_x}{\partial y}\right)$$
$$= -m_y H\frac{\partial(g\zeta + p)}{\partial x} - m_y\left(\frac{\partial h}{\partial x} - z\frac{\partial H}{\partial x}\right)\frac{\partial p}{\partial z} + \frac{\partial}{\partial x}\left(\frac{mA_v}{H}\frac{\partial u}{\partial z}\right) + Q_u \quad (1)$$

$$\frac{\partial(mHv)}{\partial t} + \frac{\partial(m_y Huv)}{\partial x} + \frac{\partial(m_x Hvv)}{\partial y} + \frac{\partial(mwv)}{\partial z} + Hu\left(mf + v\frac{\partial m_y}{\partial x} - u\frac{\partial m_x}{\partial y}\right)$$
$$= -m_x H\frac{\partial(g\zeta + p)}{\partial y} - m_x\left(\frac{\partial h}{\partial x} - z\frac{\partial H}{\partial x}\right)\frac{\partial p}{\partial z} + \frac{\partial}{\partial x}\left(\frac{mA_v}{H}\frac{\partial v}{\partial z}\right) + Q_v \quad (2)$$

$$\frac{\partial p}{\partial z} = -gH\frac{\rho - \rho_0}{\rho_0} = -gHb \quad (3)$$

$$\frac{\partial(m\zeta)}{\partial t} + \frac{\partial(m_y Hu)}{\partial x} + \frac{\partial(m_x Hv)}{\partial y} + \frac{\partial(mw)}{\partial z} = 0 \quad (4)$$

$$\frac{\partial(m\zeta)}{\partial t} + \frac{\partial\left(m_y H\int_0^1 u dz\right)}{\partial x} + \frac{\partial\left(m_x H\int_0^1 v dz\right)}{\partial y} = 0 \quad (5)$$

$$\rho = \rho(p, S, T) \quad (6)$$

$$\frac{\partial(mHS)}{\partial t} + \frac{\partial(m_y HuS)}{\partial x} + \frac{\partial(m_x HvS)}{\partial y} + \frac{\partial(mwS)}{\partial z} = \frac{\partial}{\partial z}\left(\frac{mA_b}{H}\frac{\partial S}{\partial z}\right) + Q_S \quad (7)$$

$$\frac{\partial(mHT)}{\partial t} + \frac{\partial(m_y HuT)}{\partial x} + \frac{\partial(m_x HvT)}{\partial y} + \frac{\partial(mwT)}{\partial z} = \frac{\partial}{\partial z}\left(\frac{mA_b}{H}\frac{\partial T}{\partial z}\right) + Q_T \quad (8)$$

where, u, v are the horizontal velocity components in the curvilinear coordinates (m s^{-1}), x, y are the orthogonal curvilinear coordinates in the horizontal direction (m), z is the sigma coordinate (dimensionless), t is time (s), m_x, m_y are the square roots of the diagonal components of the metric tensor (m), m is the Jacobian with $m = m_x m_y$ (m^2), p is the physical pressure in excess of the reference density hydrostatic pressure (m^2 s^{-2}), ρ_o is the reference water density (kg m^{-3}), b is the buoyancy, f is the Coriolis parameter (s^{-1}), A_v is the vertical turbulent viscosity (m^2 s^{-1}), Q_u and Q_v are the momentum source-sink terms, Q_S and Q_T are the source-sink terms for salinity and temperature, respectively, A_b is the vertical turbulent diffusivity (m^2 s^{-1}).

The Mellor-Yamada turbulent closure model connects the vertical turbulent viscosity, diffusivity with the turbulent intensity q, turbulent length scale l, and Richardson number R_q by equations (9)–(11) (Hamrick, 1992).

$$A_v = \phi_v ql = 0.4(1 + 36R_q)^{-1}(1 + 6R_q)(1 + 8R_q)ql \quad (9)$$

$$A_b = \phi_b ql = 0.5(1 + 36R_q)^{-1}ql \quad (10)$$

$$R_q = \frac{gH}{q^2}\frac{\partial b}{\partial z}\frac{l^2}{H^2} \quad (11)$$

where Φ_v and Φ_b are the stability viscosity coefficients, which account for reduced and enhanced vertical mixing or transport in stable and unstable vertically density stratified environments, respectively.

We simulated the oval-shaped Lake Arendsee (Figure 1). The computational domain, in the reference simulation, is composed of a horizontal Cartesian grid of 1,766 cells with a grid size of 50 × 50 m (Figure 1 for model grid and lake bathymetry). The vertical axis was divided into 59 layers at the deepest point using the sigma-z-coordinate grid system. This grid architecture is a new feature in EFDC and computationally more efficient than a similarly configured sigma-coordinate system (Craig, Chung, Lam, Son, & Tinh, 2014). The sigma-z-coordinate system adjusts the number of vertical layers per horizontal grid cell according to the depth below this cell. If depth variations remain relatively small, however, the total number of vertical layers is kept constant and layer thickness is adjusted. In essence, the sigma-z-coordinate system is a combination of features from sigma grids and z-grids and provides an efficient way to balance vertical resolution, allowing the horizontal gradient error in sigma grids to be reduced. We used a relatively small vertical layer thickness of 0.5 m between 5 and 15 m depth, that is, at the depth region where the metalimnion can be expected to form during summer, a layer thickness of 2 m for the surface layer (i.e. between 0 and 2 m depth), and a vertical layer thickness of 1 m elsewhere in the water column. The vertical grid was designed in this way to achieve a higher vertical resolution at the metalimnion in order to minimize numerical diffusion. This provides sufficient spatial discretization to investigate the dynamics of vertical density stratification and the corresponding gradients of vertical diffusivity. Total active wet cells amounted to 75021 cells. We further built a model with a grid size of 100 × 100 m to test the influence of the horizontal resolution of the model on the results. All parameters and the vertical configuration, in the new model, were kept unchanged and this simulation was only used for comparison, not for the climate scenarios in the study.

2.3 | Model setup and parameters

The simulation period covered the stratification period for the year 2013 and was performed from 4th April 2013 to 31st October 2013. The simulation was started on 4th April 2013, when the lake showed a homogeneous vertical temperature. The initial temperature was set to 2.51°C based on the observed value. The time step used for the model simulation was 30 s and the frequency of the simulation output was 1 hr.

Bathymetry data of the lake area with a vertical resolution of 1 m were provided by the State Agency for Flood Protection and Water Management, Saxony-Anhalt. Meteorological input data were obtained from meteorological stations at or close to the lake. Wind velocity and direction were taken from local measurements from a meteorological station located directly on the lake (Ultrasonic anemometer, EcoTech, Germany). The data for air pressure, rain, relative humidity, air temperature, solar radiation and cloud cover were obtained from the Seehausen station of the German Weather Service (DWD), about 15 km east of Lake Arendsee. All meteorological data were provided in hourly resolution.

Since the small annual inflow (water residence time > 50 years) has a negligible effect on the hydrodynamics, we excluded all inflows and outflows from our simulations. Seasonal water level fluctuations in Lake Arendsee remained within the order of a few decimeters. In order to keep the water balance of the lake constant, we excluded precipitation and evaporative loss of water in our model. However, heat loss through evaporation was included in the thermodynamic heat budget and, therefore, temperature effects from evaporation were fully accounted for.

Near the monitoring station at the deepest point of the lake, the seasonal dynamics of water temperature over the entire water body depth were measured using a thermistor logger chain containing 15 optodes (D-Opto Logger, Zebra-Tech, New Zealand). The thermistors were moored at 2.5, 5, 7.5, 10, 12.5, 15, 17.5, 20, 22.5, 25, 30, 35, 40, 45 and 48 m depths. The optodes measured temperature every hour between 28 March and 18 December 2013. The nominal accuracy of the temperature measurements was ±0.1 K with a resolution of ±0.01 K and these measurements were used for the model calibration. The main hydrodynamic and temperature parameters used in the model are listed in Table 1 and were not calibrated but just set to values common in other EFDC applications.

TABLE 1 Summary of the main model parameters used in the simulations

Parameter	Values
Background horizontal eddy viscosity	$2.5 \text{ m}^2 \text{ s}^{-1}$
Dimensionless horizontal momentum diffusivity	0.1
Background vertical eddy viscosity	$0.00001 \text{m}^2 \text{ s}^{-1}$
Background vertical molecular diffusivity	$0.0000001 \text{m}^2 \text{ s}^{-1}$
Solar radiation minimum fraction absorbed in the top layer	0.6
Background light extinction coefficient	2 m^{-1}
Bed temperature	$4°C$
Bed thermal thickness	0.1 m

2.4 | Calculation of vertical turbulent diffusion coefficient K_z

To calculate vertical diffusion coefficients, the 3D dynamic description of water temperature in a lake-averaged vertical distribution was achieved by averaging water temperature within each horizontal layer of the grid. The temporal evolution of this lake-wide vertical temperature gradient was the basis for calculating K_z by following the gradient flux method by Heinz et al. (1990), who calculated K_z based on the following equation using temperature:

$$K_z(i,t) = \frac{\sum_{k=i}^{m} \frac{\Delta T_i}{\Delta t} * V_i}{\frac{\Delta T_{i-1}}{\Delta z_i} * A_i}$$ (12)

where $K_{z,i}$ is the vertical turbulent diffusivity at the upper boundary of layer i, m refers to the deepest layer of the lake, $\frac{\Delta T_i}{\Delta t}$ is the temporal change (here: increase) in temperature, $\frac{\Delta T_{i-1}}{\Delta z}$ is the vertical gradient of temperature at the upper boundary of layer i, ΔT_{i-1} is the temperature difference between layer i-1 and i, Δz_i is the layer thickness, A_i is the area of the upper boundary and V_i is the volume of the layer.

The model-derived K_z was calculated based on Equation (12) by using the simulated water temperatures. As an alternative way to calculate K_z, a conservative (i.e. nonreactive) tracer was included in the simulation, to further test the model capability of reproducing K_z of the lake. The initial condition for the tracer vertical distribution was a linear gradient with 2 mg l^{-1} at the surface and 99 mg l^{-1} at the maximum depth of 49.5 m. The formula to calculate K_z by tracer concentrations then became:

$$K_z(i,t) = \frac{\sum_{k=i}^{m} \frac{\Delta C_i}{\Delta t} * V_k}{\frac{\Delta C_{i-1}}{\Delta z} * A_i}$$ (13)

where $\frac{\Delta C_i}{\Delta t}$ and $\frac{\Delta C_{i-1}}{\Delta z}$ are the temporal change and vertical gradient of tracer concentration at layer i. Whenever vertical mixing conditions were intense, for example, in early spring, vertical tracer gradients diminished quickly over time, making it impossible to calculate K_z. We

therefore re-established the vertical tracer concentration every 30 days and the initial tracer distribution was re-established at the start of every calculation period, that is, on 4 April, 4 May, 3 June, 3 July, 2 August, 1 September, and 1 October. EFDC allows the definition of breakpoints, where all model states are conserved, the model stops and can be reactivated by a warm start. We used this breakpoint feature every 30 days in the simulation to freeze all model states, to re-establish the vertical tracer distribution, and to proceed with the simulation for another 30 days by warm-starting from the last breakpoint. This allowed a continuous simulation of hydro-and thermodynamics while tracer distribution was re-established every month. We calculated K_z on a biweekly basis during the simulation period.

2.5 | Model performance and uncertainty analysis

Simulated and measured water temperatures, for the same time at the same depth, were compared by calculating the root-mean-squared-error (RMSE) according to Equation (14) to determine model performance.

$$RMSE = \sqrt{\frac{\sum_{i=1}^{n} (T_{i,obs} - T_{i,sim})^2}{n}}$$ (14)

We then compared our model-based vertical diffusion coefficients K_z in the metalimnion, calculated from simulated water temperatures based on Equation (12), with corresponding vertical diffusion coefficients computed in an independent study by Kreling et al. (2017), who quantified K_z at the depth of the metalimnion by using the measured water temperature according to the same equation above. Furthemore, we used the in situ K_z values computed from the thermistor data for a direct comparison with the model-based K_z over the full depth range and stratification period. Notably, in this step the simulated K_z was calculated based on different approaches (i.e. from simulated water temperatures as well as tracer concentration) and horizontal grid resolutions. We used multiple ways to calculcate model-derived vertical diffusivity in order to make our results robust against model specifications and in order to assess the uncertainty in estimated vertical diffusivity that would eventually arise from these specifications. The RMSE and values of K_z were calculated in R Statistical Software (R Core Team, 2016).

2.6 | Scenarios

We defined two scenarios for studying the effect of meteorological drivers on mixing conditions in the metalimnion. The scenarios concentrated on wind velocity and air temperature because both are highly influential for stratification dynamics and are expected to undergo changes in the future. Note that only water temperature, rather than tracer substance, was included in the scenario simulations with respect to calculating K_z:

2.6.1 | Warming scenario

Due to global warming, we expect average air temperatures to rise in a range between 1 and 4 K by the end of the century (IPCC, 2014). Although the effect of global warming on lake temperatures (O'Reilly & Sharma, 2015) and stratification (Kraemer, Anneville, & Chandra, 2015) have been thoroughly documented, its effects on the metalimnion have never been analysed in detail. We therefore simulated a simplified warming scenario by increasing air temperatures in our simulation by 2 K and analysed the mixing conditions at the thermocline.
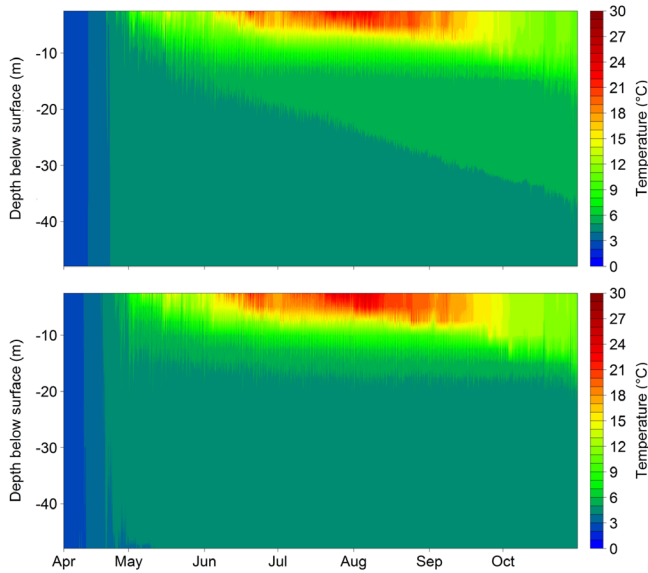
2.6.2 | Wind scenario

Future projections of wind velocity are uncertain. While the phenomenon of global wind stilling has been reported (Vautard, Cattiaux, Yiou, Thépaut, & Ciais, 2010), leading to globally declining wind velocities, other authors stress the increasing frequency of storm events (Easterling et al., 2000). Interannual variability in wind velocity is high at Lake Arendsee. For the 42-years from 1976 until 2017, for which continuous data are available from the Seehausen station, yearly averaged wind velocities varied from 2.4 to 4.1 m s^{-1} and showed a coefficient of variation of about 10%. The average wind velocity in the simulated year 2013 was 3.51 m s^{-1}, which is relatively close to the overall mean wind velocity over the 42-year period (3.56 m s^{-1}). Given the uncertainties in global projections of wind velocities, we defined the wind scenarios based on the historical observations since 1976 and varied wind by +20 and − 20% relative to the reference year 2013. This change in wind speed corresponds approximately to the 95% confidence interval of average wind conditions over the past 42 years.

3 | RESULTS

3.1 | Model performance and validity

The temporal and spatial dynamics of water temperatures in Lake Arendsee were well captured by EFDC (Figure 2) and the overall RMSE was relatively low (0.78 K). Although absolute differences between simulated and observed temperatures remained low, a systematic difference was recorded in the deep hypolimnion (i.e. at 25 m depth and below), where modelled temperatures were always higher than observations from July onwards and the difference reached 0.8 K at the end of October (Figures 2 and 3). A high RMSE of 1.76 K was observed within the metalimnion, where internal wave activity at high frequencies led to relatively large temperature variations in situ at high
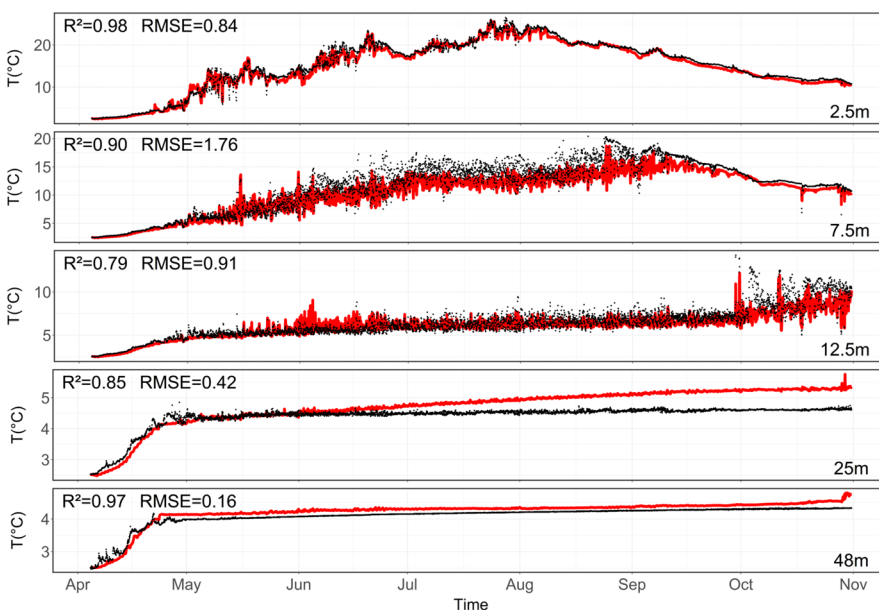

FIGURE 2 Contour plot of the simulated (above) and observed (below) water temperature in Lake Arendsee for the simulation period (04/2013–10/2013)

FIGURE 3 Simulated (red) versus observed (black) water temperatures in Lake Arendsee at different water depths (given at the right margin). The coefficient of determination and RMSE are given in the upper left corner for each depth

frequencies (Figure 3 at 7.5 m depth). The deviations between observed and simulated water temperatures at this depth reached up to 5 K. However, such large deviations were the exception and the vast majority of simulated temperatures were close to the observations (Figures 4 and S1): less than 2 ‰ of the simulated temperatures, for example, showed a deviation from observations of 5 K or more and less than 5 ‰ showed a deviation of 4 K or more. In a plot of simulated versus observed temperatures, most values closely followed the 1:1 line and the overall R^2 of the respective linear regression was about 0.98 (Figure 4). Finally, important phenomenological aspects, such as the onset of stratification or the depth of the thermocline, were properly reproduced by the model (Figure 2).

Comparing the model-based vertical diffusion coefficients K_z with the values shown in Kreling et al. (2017), it turned out that the model reproduced the magnitude of K_z in the metalimnion as well as the temporal trend of K_z over the season (Figure 5). Both model-based and measurement-derived values of K_z yielded minimal values below 1.25×10^{-6} m^2 s^{-1} in the middle of July and 5–10 times larger values
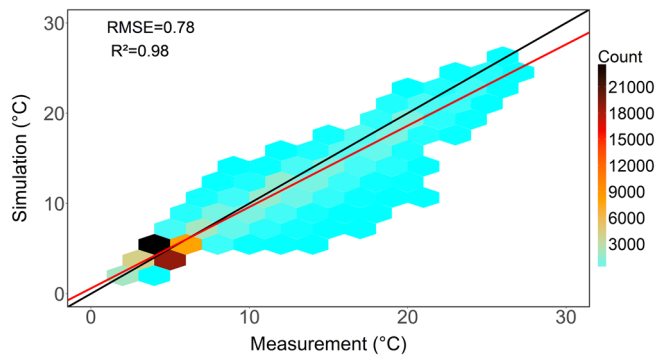

FIGURE 4   Comparison between simulated and measured water temperature for all depths (*n* = 75615). The colour bar depicts the amount of samples per hexagon. The black line has a slope of one and an intercept of zero (1:1 line). The red line shows the linear regression between the simulated and measured water temperatures in Lake Arendsee
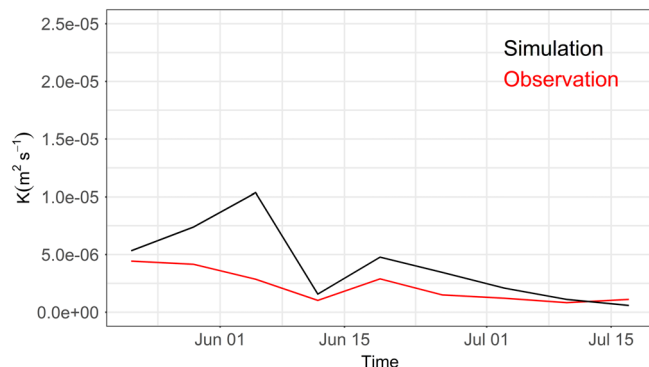

FIGURE 5   Dynamics of simulated (black) and observed (red) vertical diffusion coefficient (Kz) during summer 2013 in the metalimnion of Lake Arendsee (i.e. at the depth of the MOM, which is located at a depth of 8.2 m). Observed Kz were taken from Kreling et al. (2017) and based on in situ temperature measurements

in early summer. The agreement between the model-based and measurement-based vertical diffusion coefficient was particularly high in the 4 weeks from mid-June until mid-July, when vertical diffusion reached very low values. Before that period, that is, before June, the simulation overestimated vertical diffusion coefficients by a factor of two. Moreover, modelled K_z, calculated from water temperature as well as tracer concentration over the full depth range, followed K_z profiles from measurements during midsummer (mid-July–end of August) but showed some overestimation in early summer and early September (Figure 6). Although the model predicted a minimum of K_z within the metalimnion and the patterns appeared to be similar to field conditions, the quantitative values were systematically higher in the model during some periods and the depth of minimum K_z was shallower during early autumn. Values of K_z calculated on the basis of tracer and temperature were very close to each other (Figure 6), indicating that both methods resulted in similar estimates. Additionally, comparing results of the models with different horizontal resultions showed that grid size only marginally affected the simulated diffusivity and the vertical pattern of K_z was not sensitive to the grid resolution (Figures S2 and S3).

3.2 | Mixing conditions in the metalimnion

Observed and simulated vertical diffusion coefficients clearly indicated very low values within the metalimnion (Figure 6). The zone of low vertical exchange remained constrained over a narrow depth range that fully corresponded to the region with strong temperature gradients, and had a spatial extent of 2 to 4 m. The minimum of K_z occurred at depths between 8 and 10 m. In July, when wind velocities remained low and heating was high, the minima in vertical diffusion coefficients was most pronounced and reached values as low as 6×10^{-7} m^2 s^{-1} in our simulation. At depths 20 m and deeper, vertical diffusion coefficients were more than one order of magnitude larger than those in the metalimnion. At most times, the vertical diffusion coefficients slightly decreased towards the lake bottom so that hypolimnetic vertical diffusion showed a slight peak between 20 and 30 m depths, reaching maximum values of up to 5×10^{-5} m^2 s^{-1}.

Observed and simulated K_z in the metalimnion showed a clear seasonal development with sharply decreasing values in May, when K_z dropped from ~10^{-5} to 10^{-6} m^2 s^{-1} (Figure 7). The low values of metalimnetic K_z persisted until October (Figure 7). The location of the minimum K_z along the vertical axis also remained rather constant during the period from July until September, at depths around 8 m and moving progressively deeper thereafter due to autumnal cooling in October (Figure 8).

3.3 | Effects from changing temperature and wind conditions

The application of changing meteorological conditions with respect to wind velocity (±20%) and air temperature (+2 K) showed a high
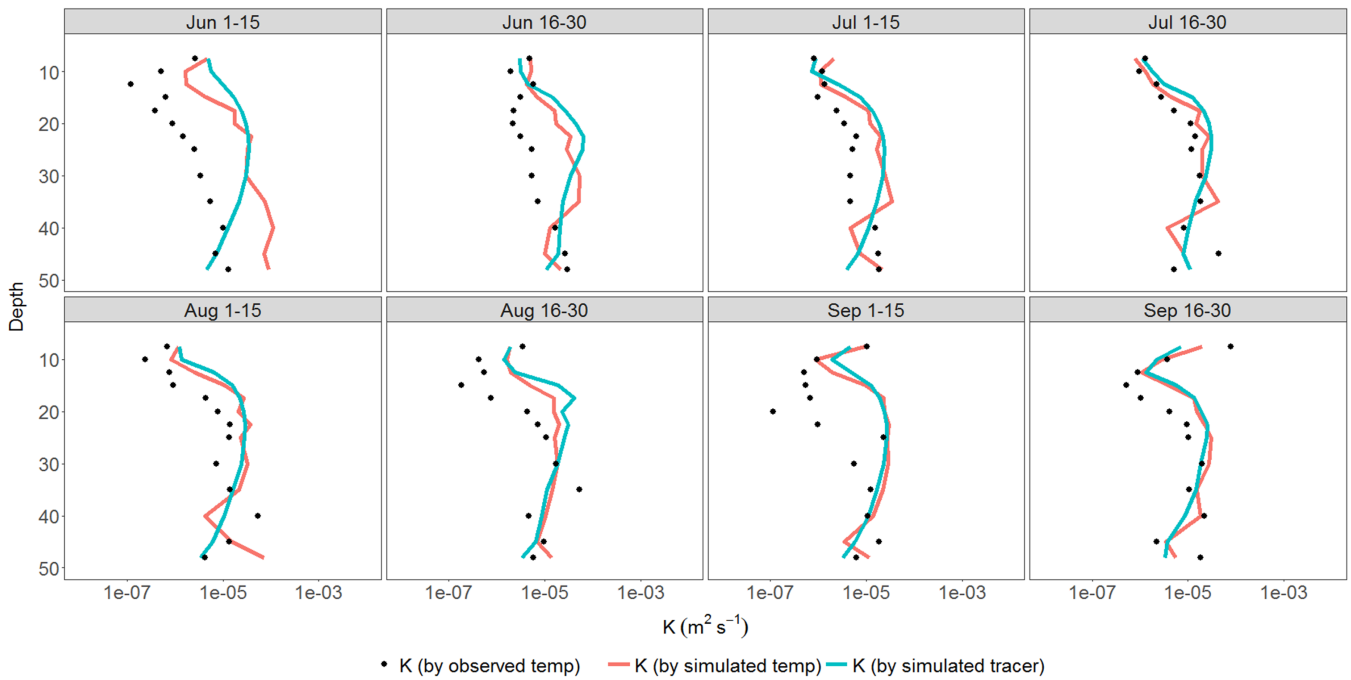
FIGURE 6 Comparison of simulated vertical diffusion coefficient Kz (derived from water temperature and tracer concentration results from the reference simulation) with observed Kz (calculated from observed water temperature dynamics) over biweekly intervals in Lake Arendsee
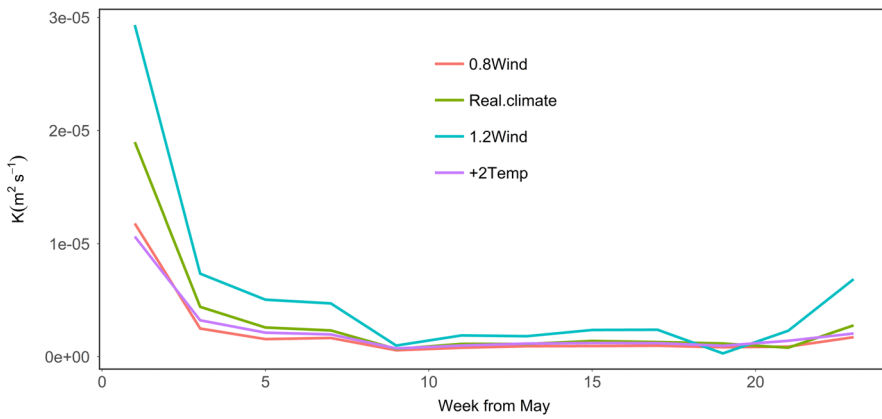

FIGURE 7 Absolute value of the minimum in vertical diffusion coefficient within the metalimnion of Lake Arendsee at different simulation scenarios with respect to wind velocity and air temperature during summer 2013
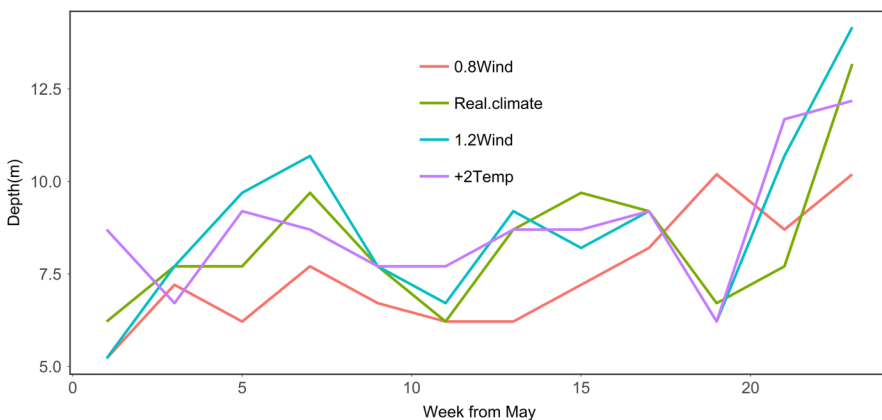

FIGURE 8 Depth of the metalimnetic minimum in vertical diffusion coefficient (as given in Figure 7) in Lake Arendsee at different simulation scenarios with respect to wind velocity and air temperature during summer 2013
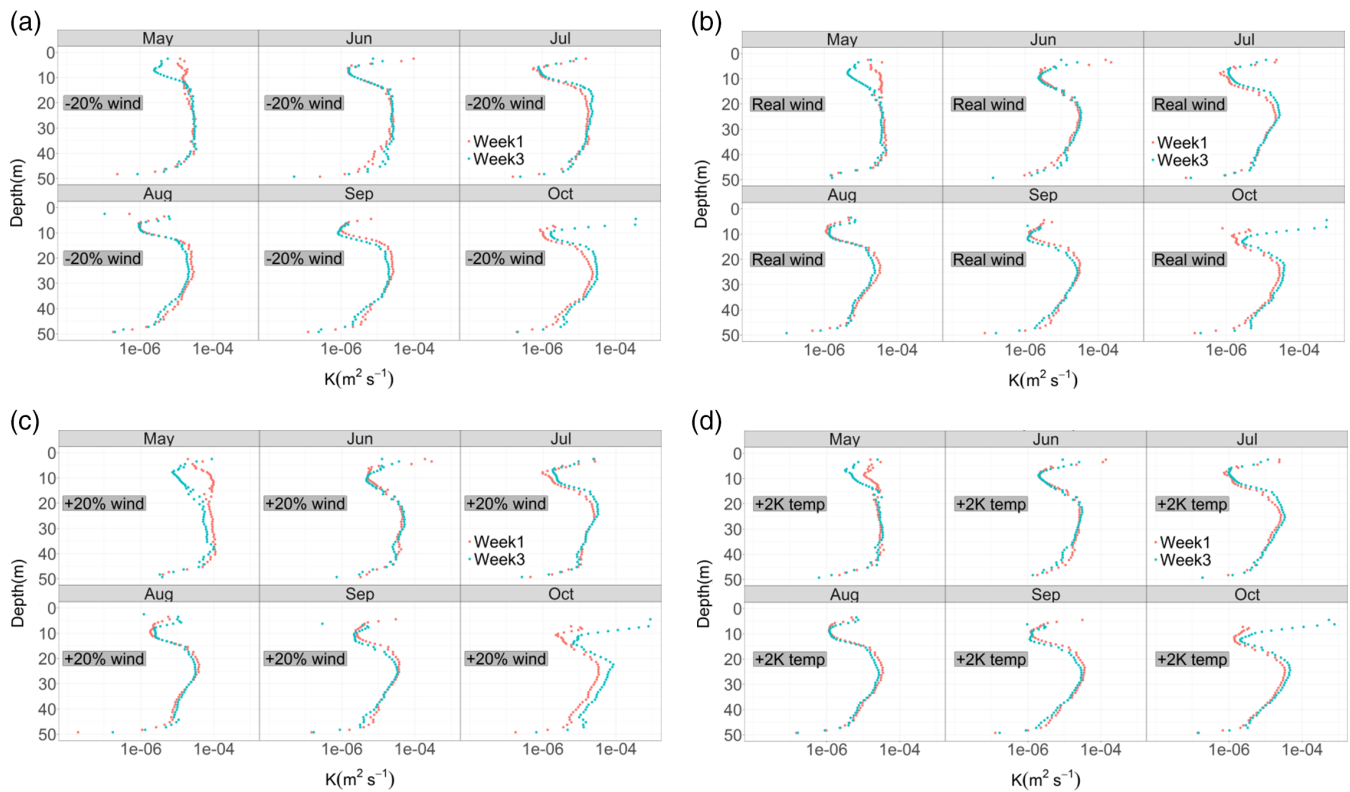
FIGURE 9 Vertical turbulent diffusivity (Kz) under different climate scenarios: (a) wind speed reduced by 20%, (b) real climate, (c) wind speed increased by 20% and (d) air temperature increased by 2 K. Values of Kz were calculated on biweekly basis (two weeks per subplot)

resistance of the metalimnetic zone, with low vertical exchange, against atmospheric forcing (Figure 9). This was particularly true for the period from July until September, when the metalimnetic vertical diffusion minimum was most pronounced. With respect to the minimal value of K_z within the metalimnion, warming and wind stilling had only marginal effects but increasing wind velocities markedly increased its value (Figure 7). At these elevated wind velocities, the duration of periods with very low vertical diffusion in the metalimnion (K_z below 5×10^{-6} m^2 s^{-1}) was notably shorter (3 weeks) than in the other scenarios. The depth of the minimal K_z in the metalimnion, however, was more sensitive to wind stilling, while warming and wind intensification did not show marked effects (Figure 8). At reduced wind velocities, the zone of low vertical exchange was about 1 to 2 m shallower than in the other scenarios. In conclusion, wind velocity appeared more influential on metalimnion depth than air temperature. While increasing wind velocities mostly affected the minimum values of K_z in the metalimnion and led to intensified vertical exchange, the reduction of wind velocity mostly affected the depth of minimal K_z but not its absolute value.

4 | DISCUSSION

4.1 | Evaluation of the modelling approach

We showed that the 3D model EFDC was able to simulate stratification dynamics in Lake Arendsee with high precision, resulting in an overall RMSE of only 0.78 K between modelled and observed water temperatures. The errors in our study were much lower than those presented in recent studies in which EFDC was applied (Bai et al., 2018; Zheng et al., 2018). The RMSE was different between layers and generally lower within the hypolimnion towards the lake bottom, which is related to lower temperature variations in this region (Figure 3). Increased discrepancies between the simulated and observed temperature profiles were only noticeable in the metaliminion, that is, at 7.5 m, from June to September (Figure 3) when the lake was strongly stratified and high internal wave activity was observed. Usually, 3D models are capable of simulating the spatiotemporal dynamics of internal waves, but this holds mostly true for basin-scale internal waves (Bocaniov, Ullmann, Rinke, Lamb, & Boehrer, 2014). The wave activity in the metalimnion of Lake Arendsee, however, showed higher frequency waves and EFDC is obviously not able to capture these high frequency phenomena. The model slightly overestimated temperatures in the hypoliminion, that is, at depth 25 and 48 m from July to October, indicating that vertical mixing in the model was higher than in reality. This turned out to be exactly the case because modelled vertical diffusion coefficients in the hypolimnion were larger than observed vertical diffusion coefficients (Figure 6). Obviously, the model has difficulty in predicting vertical diffussion properly at the start of the stratification period, when temperature gradients are not as steep as later on. Our efforts to quantify in situ K_z values, that is, the installation and evaluation of high resolution measurements of water temperature dynamics, were beneficial to the modelling process because they allowed us to link

emerging deviations between modelled and observed state variables to the underlying processes.

Our study contained three innovative points. Firstly, we evaluated our model results, not only by comparing measured and observed states (i.e. water temperature), but also by comparing results at the process level (i.e. vertical diffusion coefficients). This was a powerful approach in environmental modelling because deviations of the model outputs from observations could be attributed to specific processes. Secondly, we confirmed the ability of a 3D hydrodynamic model to realistically simulate the diffusion minima within the metalimnion, which was an important prerequisite for simulating biogeochemical gradients in the metalimnion (e.g. oxygen minima and nutrient gradients) correctly. Based on different approaches (i.e. from water temperature as well as tracer concentration), the simulated K_z followed the same patterns and the model was able to reproduce the duration and vertical extent of the metalimnetic diffusion minimum in agreement with observations, although the absolute values of K_z were sligtly overestimated in early summer and early autumn. Additionally, the model showed robust performance in capturing the observed K_z independent of the applied horizontal grid resolution (Figures S2 and S3). Thirdly, we analysed the sensitivity of the metalimnetic diffusion minimum to changing meteorological conditions. We found that wind speed had noticeable effects on vertical exchange within the metalimnion and formation of the metalimnetic diffusion minimum, while air temperature remained less influential. This is in line with the article from Magee and Wu (2017), which analysed the influence of climate changes on thermal dynamics in three lakes and found that, compared to air temperature, wind speed had a more significant effect on the stratification variables.

We used a vertical grid structure in our simulations that contained a higher resolution between 5 and 15 m depths, in order to better reproduce the conditions in the metalimnion. Vertical exchange in hydrodynamic models, that is, the vertical discretization that is used to solve the underlying partial differential equations, is dependent on this vertical resolution. The larger the vertical layers become, the greater the contribution of numerical diffusion to the overall diffusion. This is a critical issue and one may ask whether the minimum K_z within the thermocline is just a consequence of the finer grid structure at these depths. In order to rule out this concern, we repeated our simulations with a uniform grid where all layers between 2 and 50 m had a thickness of 1 m (the top layer was kept at 2 m thickness as before). It turned out that the uniform grid indeed produced slightly higher K_z values in the metalimnion (Figure S4) but the overall patterns of the vertical profiles of K_z remained similar. Hence, we concluded that the contribution of finer vertical grid structures between 5 and 15 m depths only marginally contributed to the low values in the metalimnion. In general, the vertical resolution chosen in hydrodynamic models is always influencing the effective diffusion between layers and modellers have to find a good compromise between model performance and computation time. In our case, the vertical resolution had no major effect on our results. Finally, we noted that the simulated K_z-values below the 20 m depth showed only little variation over time and the patterns seen in Figure 6 had a high self-similarity

between different biweekly periods. This observation deserves further study but probably indicates that simulated K_z in the hypolimnion are slightly but systematically overestimated and the calculation of mixing intensities in the hypolimnion by EFDC requires improvement.

4.2 | Opportunities and limits of the 3D hydrodynamic model

Three-dimensional lake models are powerful tools in hydrodynamical studies because they can account for complex spatial currents and wave patterns such as internal waves, differential cooling and upwelling. It has been shown that 3D models can realistically simulate lake-wide flow dynamics at a high spatial and temporal resolution (e.g. Appt, Imberger, & Kobus, 2004; Hodges, Imberger, Laval, & Appt, 2000). This has enabled the systematic analyses of hydrodynamical effects from wind forcing (Valerio et al., 2012), the prediction of lake wide transport processes (Hillmer, van Reenen, Imberger, & Zohary, 2008), and management-relevant water-quality dynamics to be addressed (Vilhena, Hillmer, & Hillmer, 2010). In comparison to classic 1D models, they can more realistically simulate mixing processes that involve 3D dynamics. In a study by Bocaniov et al. (2014), for example, the diapycnical mixing during a large upwelling event in a deep reservoir could be quantified. Although these features enable 3D models to account for mixing processes in a more mechanistic way, they have also been criticized for systematically overestimating mixing due to numerical diffusion (Hodges, Imberger, Saggio, & Winters, 2000), leading to the development of numerical procedures to minimize numerical diffusion (e.g. Laval, Hodges, & Imberger, 2003). Since numerical diffusion is accumulating over time, 3D models are often assumed to not be applicable when simulation times are long. Our study, however, clearly demonstrates that simulations over several seasons with a 3D model can indeed reproduce temperature dynamics and mixing intensities close to reality. The simulated K_z values in our study are mainly between 1.0×10^{-6} and 1×10^{-4} m^2 s^{-1} (Figure 6), which is within the range calculated from observed water temperature in previous studies (Imboden, Lemmin, Joller, & Schurter, 1983; Saber, James, & Hayes, 2018; Wahl & Peeters, 2014; Yang et al., 2015). However, a slight, but systematic, overestimation of hypolimnetic K_z was also visible in our study, particularly at the start of the stratified season. Obviously, EFDC could be improved by finding ways to limit numerical diffusion effects in the hypolimnion. We also observed that simulated hypolimnetic K_z peaked at depths between 20 and 30 m and slightly decreased towards the lake bottom. Observed hypolimnetic K_z, however, showed a uniform depth profile. The dynamics of physical mixing at the sediment–water interface (Wüest & Lorke, 2003), therefore, also require a more careful evaluation within EFDC.

The meteorological inputs to nearly all 3D model applications of lakes are very simplified in the sense that uniform fields of meteorological variables are applied. This seems to be a defendable assumption for temperature, radiation and humidity but in many cases not for wind, which can show quite heterogeneous spatial variations. Therefore, using homogenous wind fields to drive lake models will introduce uncertainties in the simulation results. In cases where wind fields are

far from being uniform, the application of structured wind fields (Mao, Van Der Westhuysen, Xia, Schwab, & Chawla, 2016) or the simple internal boundary layer approach (Fenocchi & Sibilla, 2016; Józsa, 2014) could be of help. We know little about the wind fields over Lake Arendsee but, given the fact that the sorrounding landscape is flat and relatively unstructured, we believe that the application of uniform wind fields in our study is an acceptable assumption.

4.3 | Limnological processes and lake ecosystem dynamics

The realistic simulation of vertical mixing is an important aspect in lake modelling because the vertical transport of nutrients or other pollutants from the sediment towards the upper water layers is a major component of internal loading. Upward transport of nutrients, for example, can drive eutrophication of lakes and reservoirs (Burger, Hamilton, & Pilditch, 2008). Similarly, the vertical downward transport of oxygen is relevant for water quality in the hypolimnion, which is of high priority in water bodies used for drinking water supply (Bryant, Hsu-Kim, Gantzer, & Little, 2011). EFDC appears to be suited for modelling these transport processes and can therefore provide a valuable tool for lake management when appropriate biogeochemical routines are included. Furthermore, since low metalimnetic turbulent diffusivity in Lake Ardensee has been shown to be a prerequisite for forming the metalimnetic oxygen minima (Kreling et al., 2017), further modelling studies should focus on the oxygen dynamics or other limnological features in the metalimnion (e.g. a deep chlorophyll maximum) and pay greater attention to a sound representation of vertical exchange within the layer. An extension of our model system by including biogeochemical routines would definitely enable us to study these phenomena in a more quantitative way and to provide predictions for lake managers.

From a lake management perspective, simulating the vertical diffusion coefficient may also help in the design of infrastructure for lake water-quality management and restoration efforts. Hypolimnetic aeration by water transfer between epi- and hypolimnion (Tian, Pan, Köngäs, & Horppila, 2017) or by bubble plume diffusers (Gantzer, Bryant, & Little, 2009) requires a quantitative estimate and solid planning for the necessary aeration intensities (Tian et al., 2017). Understanding the dynamics of vertical diffusion can provide guidance regarding the amount of aeration required and the layer of the lake to which the aeration should be applied. The model-based quantification of vertical diffusion could also help in exploring design options for the installation of hypolimnetic bubblers for thermal destratification (Moshfeghi, Etemad-Shahidi, & Imberger, 2005).

From our point of view, the metalimnion is a partly neglected compartment in lake research. In a recent study, Giling et al. (2017) pointed out that the interplay between physical drivers, chemical conditions and biological activity remained largely unresolved in this layer. The environmental conditions within the metalimnion with respect to light, temperature, or nutrients can vary from lake to lake and even within a given lake these variables change strongly within space and time and, hence, can induce complex local patterns and dynamics such as deep chlorophyll maxima (Leach et al., 2018), oxygen maxima (Wilkinson et al., 2015) or oxygen minima (Kreling et al., 2017). Apart from the case study level, generalized model-based predictions of biogeochemical activity in the metalimnion are therefore difficult to achieve. However, a special feature of the metalimnion is the very low vertical mixing intensity, making it a highly separated compartment with minimal interactions with the epilimnion above or the hypolimnion below. An important prerequisite for a thorough analysis and reliable prediction of ecological or biogeochemical activity in the metalimnion is, therefore, a sound representation of the physical conditions within this layer. Our study provides evidence that 3D models are able to capture the physical conditions in the metalimnion with reasonable precision and therefore provide a fundament for a more systematic understanding of the ecological dynamics within this fascinating lake compartment.

5 | CONCLUSION

In this study, we comprehensively evaluated the performance of a well-established 3D hydrodynamic model (EFDC) in capturing the stratification and mixing dynamics of Lake Arendsee. In parallel to the model simulations, we established high frequency monitoring of stratification dynamics that enabled us to compute vertical turbulent diffusion coefficients (K_z) from in situ measurements. The results showed that our model can not only accurately reproduce water temperatures, but can also realistically simulate vertical gradients of K_z within the lake. Moreover, the model predictions regarding the duration and vertical extent of the metalimnetic diffusion minimum were robust with respect to model grid resolution and calculation of K_z (from numerical tracer distribution or from simulated water temperature). Through a scenario analysis we further illustrated the influence of changing meteorological conditions on the metalimnetic diffusion minimum. Wind speed was shown to be a more influential factor for the spatio-temporal development of the diffusion minimum than air temperature. While increasing wind velocities mostly affected the minimum values of K_z in the metalimnion, wind stilling mostly affected the depth of minimal K_z but not its absolute value. Since low metalimnetic turbulent diffusivity is a prerequisite for the formation of oxygen minima and chlorophyll maxima in the layer, it is recommended that further modelling studies take such biological processes into account in order to obtain a full perspective on the topic.

DATA AVAILABILITY STATEMENT

The data that support the findings of this study are available from the corresponding author upon reasonable request.

ORCID

Chenxi Mi https://orcid.org/0000-0003-2323-1832
Karsten Rinke https://orcid.org/0000-0003-0864-6722

REFERENCES

Appt, J., Imberger, J., & Kobus, H. (2004). Basin-scale motion in stratified Upper Lake Constance. *Limnology and Oceanography*, *49*, 919–933.

Arhonditsis, G. B., & Brett, M. T. (2004). Evaluation of the current state of mechanistic aquatic biogeochemical modeling. *Marine Ecology Progress Series*, *271*, 13–26.

Bai, H., Chen, Y., Wang, D., Zou, R., Zhang, H., Ye, R., ... Sun, Y. (2018). Developing an EFDC and numerical source-apportionment model for nitrogen and phosphorus contribution analysis in a Lake Basin. *Water*, *10*, 1315.

Bernhardt, J., & Kirillin, G. (2013). Seasonal pattern of rotation-affected internal seiches in a small temperate lake. *Limnology and Oceanography*, *58*, 1344–1360.

Bocaniov, S. A., Ullmann, C., Rinke, K., Lamb, K. G., & Boehrer, B. (2014). Internal waves and mixing in a stratified reservoir: insights from three-dimensional modeling. *Limnologica*, *49*, 52–67.

Boehrer, B. (2000). Modal response of a deep stratified lake: western Lake Constance. *Journal of Geophysical Research: Oceans*, *105*, 28837–28845.

Boehrer, B., Ilmberger, J., & Münnich, K. O. (2000). Vertical structure of currents in western Lake Constance. *Journal of Geophysical Research: Oceans*, *105*, 28823–28835.

Boehrer, B. & Schultze, M. (2008). Stratification of lakes. Reviews of Geophysics 46:RG 2005.

Bryant, L. D., Hsu-Kim, H., Gantzer, P. A., & Little, J. C. (2011). Solving the problem at the source: Controlling Mn release at the sediment-water interface via hypolimnetic oxygenation. *Water Research*, *45*, 6381–6392.

Burger, D. F., Hamilton, D. P., & Pilditch, C. A. (2008). Modelling the relative importance of internal and external nutrient loads on water column nutrient concentrations and phytoplankton biomass in a shallow polymictic lake. *Ecological Modelling*, *211*, 411–423.

Craig, P., Chung, D., Lam, N., Son, P. & Tinh, N., 2014. *Sigma-zed: A computationally efficient approach to reduce the horizontal gradient error in the EFDC's vertical sigma grid*. ICHD.

Dietz, S., Lessmann, D., & Boehrer, B. (2012). Contribution of solutes to density stratification in a meromictic lake (Waldsee/Germany). *Mine Water and the Environment*, *31*, 129–137.

Easterling, D. R., Meehl, G. A., Parmesan, C., Changnon, S. A., Karl, T. R., & Mearns, L. O. (2000). Climate extremes: observations, modeling, and impacts. *Science*, *289*, 2068–2074.

Engelhardt, C., & Kirillin, G. (2014). Criteria for the onset and breakup of summer lake stratification based on routine temperature measurements. *Fundamental and Applied Limnology/Archiv für Hydrobiologie*, *184*, 183–194.

Fenocchi, A., Rogora, M., Morabito, G., Marchetto, A., Sibilla, S., & Dresti, C. (2019). Applicability of a one-dimensional coupled ecological-hydrodynamic numerical model to future projections in a very deep large lake (Lake Maggiore, Northern Italy/Southern Switzerland). *Ecological Modelling*, *392*, 38–51.

Fenocchi, A., & Sibilla, S. (2016). Hydrodynamic modelling and characterisation of a shallow fluvial lake: a study on the Superior Lake of Mantua. *Journal of Limnology*, *75*.

Findlay, D., Kling, H., Rönicke, H., & Findlay, W. (1998). A paleolimnological study of eutrophied Lake Arendsee (Germany). *Journal of Paleolimnology*, *19*, 41–54.

Frassl, M. A., Boehrer, B., Holtermann, P. L., Hu, W., Klingbeil, K., Peng, Z., ... Rinke, K. (2018). Opportunities and limits of using meteorological reanalysis data for simulating seasonal to sub-daily water temperature dynamics in a large shallow lake. *Water*, *10*, 594.

Gantzer, P. A., Bryant, L. D., & Little, J. C. (2009). Effect of hypolimnetic oxygenation on oxygen depletion rates in two water-supply reservoirs. *Water Research*, *43*, 1700–1710.

Gaudard, A., Schwefel, R., Vinnå, L. R., Schmid, M., Wüest, A., & Bouffard, D. (2017). Optimizing the parameterization of deep mixing and internal seiches in one-dimensional hydrodynamic models: A case study with Simstrat v1. 3. *Geoscientific Model Development*, *10*, 3411–3423.

Giling, D. P., Staehr, P. A., Grossart, H. P., Andersen, M. R., Boehrer, B., Escot, C., ... Jones, I. D. (2017). Delving deeper: Metabolic processes in the metalimnion of stratified lakes. *Limnology and Oceanography*, *62*, 1288–1306.

Goudsmit, G. H., Peeters, F., Gloor, M., & Wüest, A. (1997). Boundary versus internal diapycnal mixing in stratified natural waters. *Journal of Geophysical Research: Oceans*, *102*, 27903–27914.

Hamrick, J. M. (1992). *A three-dimensional environmental fluid dynamics computer code: Theoretical and computational aspects*.

Hamrick, J. M. (1996). *User's manual for the environmental fluid dynamics computer code*.

Heinz, G., Ilmberger, J., & Schimmele, M. (1990). Vertical mixing in Überlinger See, western part of Lake Constance. *Aquatic Sciences*, *52*, 256–268.

Hillmer, I., van Reenen, P., Imberger, J., & Zohary, T. (2008). Phytoplankton patchiness and their role in the modelled productivity of a large, seasonally stratified lake. *Ecological Modelling*, *218*, 49–59.

Hodges, B., Imberger, J., Laval, B., & Appt, J. (2000). Modeling the hydrodynamics of stratified lakes. In *Hydroinformatics 2000 conference* (Vol. 4) (pp. 23–27).

Hodges, B. R., Imberger, J., Saggio, A., & Winters, K. B. (2000). Modeling basin-scale internal waves in a stratified lake. *Limnology and Oceanography*, *45*, 1603–1620.

Hupfer, M., Reitzel, K., Kleeberg, A., & Lewandowski, J. (2016). Long-term efficiency of lake restoration by chemical phosphorus precipitation: Scenario analysis with a phosphorus balance model. *Water Research*, *97*, 153–161.

Imberger, J. (1981). A dynamic reservoir simulation model-DYRESM. *Transport Models for Inland and Coastal Waters*, 310–361.

Imboden, D. M., Lemmin, U., Joller, T., & Schurter, M. (1983). MIXING PROCESSES IN LAKES - MECHANISMS AND ECOLOGICAL RELEVANCE. *Schweizerische Zeitschrift Fur Hydrologie-Swiss Journal of Hydrology*, *45*, 11–44.

IPCC (2014). Climate change 2014: Synthesis report. Contribution of Working Groups I,II and III to the fifth assessment report of the intergovernmental panel on climate change. In Core Writing Team, R. K. Pachauri, & L. A. Meyer (Eds.), (p. 151). Geneva, Switzerland: IPCC.

Józsa, J. (2014). On the internal boundary layer related wind stress curl and its role in generating shallow lake circulations. *Journal of Hydrology and Hydromechanics*, *62*, 16–23.

Kraemer, B. M., Anneville, O., & Chandra, S. (2015). Morphometry and average temperature affect lake stratification responses to climate change. *Geophysical Research Letters*, *42*, 4981–4988.

Kreling, J., Bravidor, J., Engelhardt, C., Hupfer, M., Koschorreck, M., & Lorke, A. (2017). The importance of physical transport and oxygen consumption for the development of a metalimnetic oxygen minimum in a lake. *Limnology and Oceanography*, *62*, 348–363.

Laval, B., Hodges, B. R., & Imberger, J. (2003). Reducing numerical diffusion effects with pycnocline filter. *Journal of Hydraulic Engineering*, *129*, 215–224.

Leach, T. H., Beisner, B. E., Carey, C. C., Pernica, P., Rose, K. C., Huot, Y., … Ibelings, B. W. (2018). Patterns and drivers of deep chlorophyll maxima structure in 100 lakes: The relative importance of light and thermal stratification. *Limnology and Oceanography*, *63*, 628–646.

Lehner, B., & Döll, P. (2004). Development and validation of a global database of lakes, reservoirs and wetlands. *Journal of Hydrology*, *296*, 1–22.

Luo, Y., Zhao, Y., Yang, K., Chen, K., Pan, M., & Zhou, X. (2018). Dianchi Lake watershed impervious surface area dynamics and their impact on lake water quality from 1988 to 2017. *Environmental Science and Pollution Research*, *25*, 29643–29653.

Magee, M. R., & Wu, C. H. (2017). Response of water temperatures and stratification to changing climate in three lakes with different morphometry. *Hydrology and Earth System Sciences*, *21*, 6253–6274.

Mao, M., Van Der Westhuysen, A. J., Xia, M., Schwab, D. J., & Chawla, A. (2016). Modeling wind waves from deep to shallow waters in Lake Michigan using unstructured SWAN. *Journal of Geophysical Research: Oceans*, *121*, 3836–3865.

Meinikmann, K., Hupfer, M., & Lewandowski, J. (2015). Phosphorus in groundwater discharge–A potential source for lake eutrophication. *Journal of Hydrology*, *524*, 214–226.

Mellor, G. L., & Yamada, T. (1982). Development of a turbulence closure model for geophysical fluid problems. *Reviews of Geophysics*, *20*, 851–875.

Mi, C., Frassl, M. A., Boehrer, B., & Rinke, K. (2018). Episodic wind events induce persistent shifts in the thermal stratification of a reservoir (Rappbode Reservoir, Germany). *International Review of Hydrobiology*, *103*, 71–82.

Mi, C., Sadeghian, A., Lindenschmidt, K.-E., & Rinke, K. (2019). Variable withdrawal elevations as a management tool to counter the effects of climate warming in Germany's largest drinking water reservoir. *Environmental Sciences Europe*, *31*, 19.

Moshfeghi, H., Etemad-Shahidi, A., & Imberger, J. (2005). Modelling of bubble plume destratification using DYRESM. *Journal of Water Supply: Research and Technology-AQUA*, *54*, 37–46.

O'Reilly, C. M., & Sharma, S. (2015). Rapid and highly variable warming of lake surface waters around the globe. *Geophysical Research Letters*, *42*, 10773–10781.

Peeters, F., Straile, D., Lorke, A., & Ollinger, D. (2007). Turbulent mixing and phytoplankton spring bloom development in a deep lake. *Limnology and Oceanography*, *52*, 286–298.

Pekel, J.-F., Cottam, A., Gorelick, N., & Belward, A. S. (2016). High-resolution mapping of global surface water and its long-term changes. *Nature*, *540*, 418.

Perroud, M., Goyette, S., Martynov, A., Beniston, M., & Anneville, O. (2009). Simulation of multiannual thermal profiles in deep Lake Geneva: A comparison of one-dimensional lake models. *Limnology and Oceanography*, *54*, 1574–1594.

Riley, M. J., & Stefan, H. G. (1988). MINLAKE: A dynamic lake water quality simulation model. *Ecological Modelling*, *43*, 155–182.

Saber, A., James, D. E., & Hayes, D. F. (2018). Effects of seasonal fluctuations of surface heat flux and wind stress on mixing and vertical diffusivity of water column in deep lakes. *Advances in Water Resources*, *119*, 150–163.

Sommer, U., Gliwicz, Z. M., Lampert, W., & Duncan, A. (1986). The PEG-model of seasonal succession of planktonic events in fresh waters. *Archiv für Hydrobiologie*, *106*, 433–471.

Stepanenko, V. M., Goyette, S., Martynov, A., Perroud, M., Fang, X., & Mironov, D. (2010). First steps of a Lake Model Intercomparison Project: LakeMIP. *Boreal Environment Research*, *15*, 191–202.

Team, R. C. (2016). *R: A language and environment for statistical computing*. Vienna, Austria: R Foundation for Statistical Computing.

Tetra, T. (2007). *The environmental fluid dynamics code theory and computation volume 3: Water quality module*. VA: Fairfax.

Tian, X., Pan, H., Köngäs, P., & Horppila, J. (2017). 3D-modelling of the thermal circumstances of a lake under artificial aeration. *Applied Water Science*, 1–8.

Valerio, G., Pilotti, M., Marti, C. L., & Imberger, J. r. (2012). The structure of basin-scale internal waves in a stratified lake in response to lake bathymetry and wind spatial and temporal distribution: Lake Iseo, Italy. *Limnology and Oceanography*, *57*, 772–786.

Vautard, R., Cattiaux, J., Yiou, P., Thépaut, J.-N., & Ciais, P. (2010). Northern Hemisphere atmospheric stilling partly attributed to an increase in surface roughness. *Nature Geoscience*, *3*, 756.

Vilhena, L. C., Hillmer, I., Hillmer, I., & Imberger, J. (2010). The role of climate change in the occurrence of algal blooms: Lake Burragorang, Australia. *Limnology and Oceanography*, *55*, 1188–1200.

Wahl, B., & Peeters, F. (2014). Effect of climatic changes on stratification and deep-water renewal in Lake Constance assessed by sensitivity studies with a 3D hydrodynamic model. *Limnology and Oceanography*, *59*, 1035–1052.

Wang, Q., Li, S., Jia, P., Qi, C., & Ding, F. (2013). A review of surface water quality models. *The Scientific World Journal*, *2013*.

Wentzky, V. C., Frassl, M. A., Rinke, K., & Boehrer, B. (2019). Metalimnetic oxygen minimum and the presence of Planktothrix rubescens in a low-nutrient drinking water reservoir. *Water Research*, 208–218.

Wilkinson, G. M., Cole, J. J., Pace, M. L., Johnson, R. A., & Kleinhans, M. J. (2015). Physical and biological contributions to metalimnetic oxygen maxima in lakes. *Limnology and Oceanography*, *60*, 242–251.

Woolway, R. I., & Merchant, C. J. (2017). Amplified surface temperature response of cold, deep lakes to inter-annual air temperature variability. *Scientific Reports*, *7*, 4130.

Wu, G., & Xu, Z. (2011). Prediction of algal blooming using EFDC model: Case study in the Daoxiang Lake. *Ecological Modelling*, *222*, 1245–1252.

Wüest, A., & Lorke, A. (2003). Small-scale hydrodynamics in lakes. *Annual Review of Fluid Mechanics*, *35*, 373–412.

Yang, K., Yu, Z., Luo, Y., Yang, Y., Zhao, L., & Zhou, X. (2018). Spatial and temporal variations in the relationship between lake water surface temperatures and water quality-A case study of Dianchi Lake. *Science of the Total Environment*, *624*, 859–871.

Yang, P., Xing, Z., Fong, D. A., Monismith, S. G., Tan, K. M., & Lo, E. Y. (2015). Observations of vertical eddy diffusivities in a shallow tropical reservoir. *Journal of Hydro-Environment Research*, *9*, 441–451.

Yeates, P., & Imberger, J. (2003). Pseudo two-dimensional simulations of internal and boundary fluxes in stratified lakes and reservoirs. *International Journal of River Basin Management*, *1*, 297–319.

Zheng, H., Lei, X., Shang, Y., Duan, Y., Kong, L., Jiang, Y., & Wang, H. (2018). Sudden water pollution accidents and reservoir emergency operations: impact analysis at Danjiangkou Reservoir. *Environmental Technology*, *39*, 787–803.

SUPPORTING INFORMATION

Additional supporting information may be found online in the Supporting Information section at the end of this article.